Weakly Nonlinear Model for Oscillatory Instability in Saturn's Dense Rings

Jürgen Schmidt[1] and Heikki Salo[2]

[1]*University of Potsdam, Department of Physics, Postfach 601553, D-14415 Potsdam, Germany*
[2]*Department of Physical Sciences, Division of Astronomy, University of Oulu, Finland*

(Received 25 October 2002; published 14 February 2003)

Viscous overstability (oscillatory instability) may play an important role in the formation of small scale structure in dense planetary rings such as Saturn's *B* ring. We investigate the growth and saturation of such modes in local particle simulations. Starting from a hydrodynamic model, we develop a set of ordinary differential equations to model the evolution of the amplitudes of the linearly overstable modes in the nonlinear regime. The NASA/ESA space probe Cassini can make direct observations of these modes in Saturn's rings, including their sizes and temporal development.

DOI: 10.1103/PhysRevLett.90.061102 PACS numbers: 96.30.Wr, 45.70.Mg, 45.70.Qj, 96.30.Mh

One of the long-standing problems of the dynamics of planetary rings is the formation of the complex structure in Saturn's ring system. In the Voyager data the *B* ring exhibits radial structure on scales from thousands of kilometers to a few hundred meters [1,2]. A number of mechanisms that sculpture the ring system have been described in the literature [3–6] but undoubtedly the bulk of the structure in the *B* ring remains unexplained. It has also been shown that a *diffusive instability* of viscous origin [7,8] does not work in the rings [9,10]. On the other hand, an *oscillatory instability* of viscous origin (viscous overstability) has been proposed in the literature [11,12]. Recently we confirmed overstability directly in dynamical particle simulations [13], for parameters (particle size, material properties) falling in the midst of the plausible values for Saturn's *B* ring. Thus overstability is a promising candidate to explain structure in dense rings. For a comparison to observations it is important to study the nonlinear development of the oscillatory modes, to understand the saturation of the growth, saturation amplitudes, and their nonlinear interaction. For example, in our simulations we observe that linearly unstable radial perturbations, with typical initial lengths of hundreds of meters, are gradually displaced by longer modes. The imaging and occultation experiments on board the NASA/ESA space mission CASSINI, arriving at Saturn in 2004, will provide a test for the model. Density scans and imaging of the rings under various geometries belong to the central objectives of the mission [14,15].

In this Letter we develop a weakly nonlinear model to describe the saturation of linearly unstable oscillatory modes of the particle flow. Saturn's dense rings, consisting of meter-sized dissipatively colliding ice particles, form in principle a granular flow. Our model is derived from the basic balance equations for momentum and mass using the method of multiple scales [16]. We compare the model to direct particle simulations, simulating a patch of a planetary ring, using a periodic box of inelastic, identical, spherical, meter-sized particles. For the coefficient of restitution we employ a velocity dependent expression determined experimentally from collisions of ice spheres [17]. Details on the simulation method can be found in [10,18]. The radial length of the simulation box is typically about a hundred meters to a few kilometers. We approximate the ring's self-gravity by enhancing the frequency of vertical oscillations. This means that in the particles' equations of motion, in the component $F_z = -\Omega^2 z$ of the central gravity perpendicular to the ring, the Keplerian frequency Ω is replaced by $\Omega_z = 2\Omega$. This factor flattens the ring and increases the collision frequency in a similar way as direct gravity does, and, most importantly, it leads to a very similar overstable behavior, while being computationally much faster. It has to be noted however, that true particle-particle gravity leads to additional effects, such as gravitational wakes [13,19]. Using the frequency enhancement is an approximation that allows for an analytically treatable nonlinear model of the basic effect and the simulation of dense overstable systems over thousands of orbits.

The optical depth τ of a planetary ring can be directly observed [1,20]. It is defined as the total cross section of the particles divided by the area of the ring, i.e., $\tau = \pi r^2 n$ for a system of identical particles of radius r with surface number density n. The dense *B* ring has optical depths from 0.8 up to 2.5 at least.

In Fig. 1 results from a simulation with $\tau = 1.4$ are shown. In a simulation box with a radial width of 300 particle radii (meters) oscillatory modes form spontaneously (in this example we start from small seed perturbations). The plot shows the evolution of the surface density profile and the Fourier amplitudes of the radial oscillations in the radial velocity. Fastest growing is the perturbation with a wavelength of 100 m, but it is displaced by the more slowly growing 150 m mode, which is in turn displaced by the 300 m mode. This process would continue, if the box width allowed for the growth of larger wavelengths. Also we observe a transition from standing waves (which were seeded) to a traveling wave.

In what follows, we derive a weakly nonlinear model for overstable modes. The evolution of surface density σ and planar velocity field $\vec{u} = \{u, v\}$ is

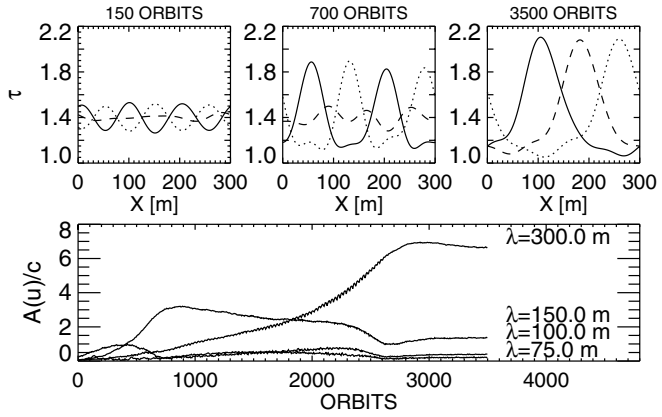

FIG. 1. Upper panel: Time evolution of the radial density profile in a simulation. Three profiles separated by a quarter orbital period are shown at three stages of the dynamical evolution. Lower panel: Fourier amplitudes of mean radial velocities.

$$(\partial_t + u_i\partial_i)\sigma = -\sigma\partial_i u_i, \tag{1}$$

$$\sigma(\partial_t + u_i\partial_i)u_j = \sigma F_j - \partial_i \hat{P}_{ij}, \tag{2}$$

where $\vec{F}$ is the central gravity force. The pressure tensor is assumed to have Newtonian form

$$\hat{P}_{ij} = p\delta_{ij} - \eta\left(\partial_i u_j + \partial_j u_i - \frac{2}{3}\delta_{ij}\partial_k u_k\right) + \xi\delta_{ij}\partial_k u_k, \tag{3}$$

with the dynamic shear and bulk viscosities η and ξ. We use a frame rotating around a planet of mass M at a radial distance a, with angular velocity $\Omega = \sqrt{GM/a^3}$. The x axis points radially outward and y is the direction of orbital motion. The planet's gravity is linearized in powers of x/a and y/a. We express time in units of the orbital frequency and surface density in terms of the uniform ground state surface density Σ. Velocities are scaled with the *effective* velocity dispersion c of the system, defined via the total pressure of the ground state $p = c^2\Sigma$ (including the collisional contributions, dominant in dense particle systems). We use specific assumptions for the density dependence of the pressure and the transport coefficients. So, for the *dynamic* shear viscosity the power law $\eta = \nu\sigma^{1+\beta}$ is employed, where ν denotes the dimensionless *kinematic* shear viscosity of the unperturbed state. It is assumed that bulk viscosity (the *kinematic* ground state value denoted by ζ) has the same dependence on surface density. For the pressure we assume $p' = \sigma'\partial p/\partial\sigma$ and write $p_\sigma = \partial p/\partial\sigma$. Restricted to radial perturbations the dimensionless balance Eqs. (1) and (2) in the corotating frame read

$$\dot{\sigma} = -(\sigma u)', \tag{4}$$

$$\dot{u} = 2v - p_\sigma\frac{\sigma'}{\sigma} - uu' + \alpha\frac{\nu}{\sigma}(\sigma^{\beta+1}u')', \tag{5}$$

$$\dot{v} = -\frac{u}{2} - uv' + \frac{\nu}{\sigma}\left(\sigma^{\beta+1}\left[v' - \frac{3}{2}\right]\right)', \tag{6}$$

where $\alpha = 4/3 + \zeta/\nu$. The tangential velocity component v is the *deviation* from local Keplerian shear $-3x/2$. The dotted terms denote time derivatives and a prime the derivative with respect to the radial coordinate. Equations (4)–(6) have the stationary solution

$$\sigma_0 = 1, \qquad u_0 = 0, \qquad v_0 = 0, \tag{7}$$

describing a uniform flow with a linear shear profile.

In total, our model has the parameters ν, α, β, and p_σ. It has been shown in the literature [11,21] that for parameters β larger than a critical value β_{cr} the ground state (7) has linearly unstable oscillatory modes. We use the method of multiple scales [16] to follow near criticality the slow evolution of these modes in the nonlinear regime. With the reduced order parameter $\delta^2 = (\beta - \beta_{cr})/\beta_{cr}$ we define the slow time scale $\theta = \delta^2 t$, replacing $\partial_t \to \partial_t + \delta^2\partial_\theta$, and expand the vector of state variables $\psi(x, t, \theta) = \{\sigma, u, v\}$ and β as

$$\psi(x, t, \theta) = \sum_{i=0}^{\infty}\delta^i\psi_i(x, t, \theta),$$
$$\beta = \beta_{cr} + \delta\beta_1 + \delta^2\beta_2 + \ldots \tag{8}$$

to obtain from (4)–(6)

$$\begin{aligned} &O(\delta^1): L\psi_1 = 0, \\ &O(\delta^2): L\psi_2 = N_2(\psi_1, \psi_1), \\ &O(\delta^3): L\psi_3 = N_3(\psi_1, \psi_2) + \partial_\theta\psi_1, \end{aligned} \tag{9}$$

with the linear operator

$$L = \begin{pmatrix} \partial_t & \partial_x & 0 \\ p_\sigma\partial_x & \partial_t - \alpha\nu\partial_x^2 & -2 \\ \frac{3}{2}\nu(1+\beta_{cr})\partial_x & \frac{1}{2} & \partial_t - \nu\partial_x^2 \end{pmatrix}. \tag{10}$$

For each order i the N_i are nonlinear functions of the solutions of the lower order equations. The first order in the sequence of Eqs. (9) yields for radial excitations $\psi_1 \propto \exp\{st + ikx\}$ the dispersion relation

$$\begin{aligned} 0 = {} & s^3 + s^2k^2\nu(1+\alpha) + s(1 + p_\sigma k^2 + k^4\nu^2\alpha) \\ & + \nu k^2[3(1+\beta) + k^2 p_\sigma]. \end{aligned} \tag{11}$$

From this we obtain the marginal curve

$$\beta_{cr}(k) = \frac{1}{3}(\alpha - 2) + \frac{1}{3}\alpha(p_\sigma k^2 + [1+\alpha]\nu^2 k^4), \tag{12}$$

the system being overstable for $\beta > \beta_{cr}(k)$.

Fredholm's theorem [16] states that solutions of the inhomogeneous linear problem exist if and only if the inhomogeneity is orthogonal to the solutions φ_0^{ad} of the homogeneous adjoint problem [22]. The scalar product of Eqs. (9) with φ_0^{ad} yields the solvability conditions

$$O(\delta^2): \langle\varphi_0^{ad}|N_2(\psi_1, \psi_1)\rangle = 0, \tag{13}$$

TABLE I. Dimensionless parameters for the coefficients of the amplitude equations. The Keplerian frequency used for the scaling is $\Omega = 1.948 \times 10^{-4}$ s^{-1}, corresponding to a location in Saturn's B ring at a distance of 100 000 km of the planet.

τ	Ω_z/Ω	c (cm/s)	β	ν	α	p_σ	α^{eff}	p_σ^{eff}
1.0	2.0	0.050	0.85	0.345	3.65	1.87	5.70	2.08
1.4	2.0	0.058	1.03	0.351	3.41	2.07	4.92	1.86
1.5	2.0	0.060	1.06	0.350	3.40	2.11	4.80	1.85
2.0	2.0	0.071	1.16	0.345	3.33	2.26	4.75	1.98

$$O(\delta^3):\langle\varphi_0^{\text{ad}}|N_3(\psi_1,\psi_2) + \partial_\theta\psi_1\rangle = 0. \quad (14)$$

The condition for order δ^3 determines the time development of the solution ψ_1 on the slow time scale θ. We take as a solution to linear order a superposition of marginally stable left and right traveling waves

$$\psi_1 = \tilde{A}_R(\theta)\varphi(k)e^{-i\omega t+ikx} + \tilde{A}_L(\theta)\varphi(-k)e^{-i\omega t-ikx} + \text{c.c.} \quad (15)$$

with amplitude functions $\tilde{A}_R(\theta)$, $\tilde{A}_L(\theta)$, and

$$\varphi = [\nu k^2 - i\omega](2ik, 2i\omega, 1 + \alpha\nu k^2[\nu k^2 + i\omega]), \quad (16)$$

which is an eigenfunction of the linear operator (10). We have $\omega = \sqrt{1 + p_\sigma k^2 + \alpha\nu^2 k^4}$ as the frequency of oscillations at marginal stability. Using ψ_1 we compute N_2 and find that the solvability condition at this order requires simply $\beta_1 = 0$ which in turn affords $\beta_2 = \beta_{\text{cr}} + O(\delta^3)$.

It is straightforward, yet lengthy, to compute a solution ψ_2. With ψ_2 the solvability condition at third order is

$$\partial_t A_R = \delta^2 g A_R - l_1|A_R|^2 A_R - l_2|A_L|^2 A_R \quad (17)$$

for A_R and for $A_L \leftrightarrow A_R$ an analogous equation, expressed here in unscaled units $\delta^2\partial_\theta = \partial_t$ and $\delta\tilde{A} = A$.

The solvability condition yields explicit expressions for the complex coefficients g, l_1, l_2 depending on the model parameters $\alpha, \beta, \nu, p_\sigma$, and k. We have determined the latter set of parameters from simulations [13] and have shown that a *nonisothermal* model describes well the linear instability of overstable modes in simulations [21]. The inclusion of the energy balance equation leads to a significant stabilization of the system, in agreement to those simulations [21]. Thus in principle the full set of equations should be used, which however, leads to a considerable complication of the model. Nevertheless, from the growth rates of the linearized nonisothermal model (see Eq. 24 of [21]), we can easily construct effective values for α and p_σ, so that the *isothermal* model (4)–(6), using the effective values, has the same growth rates. Four sets of parameters are displayed in Table I. The system with $\tau = 1$ is stable, $\tau = 1.4, 1.5, 2.0$ are overstable. For $\tau = 1.4$ the real parts of the coefficients of the Landau equations (17) are shown in Fig. 2.

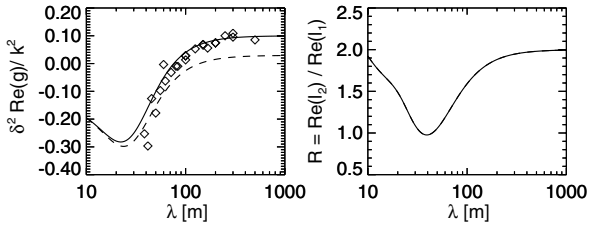

FIG. 2. Real parts of the coefficients of the Landau equations. Left panel: Growth rates of the linear theory (dashed line: parameters for $\tau = 1.4$ from Table I, solid line: 13% enhanced β). Symbols: Growth rates determined from overstable simulations. Right panel: Theoretical $\text{Re}(l_2)/\text{Re}(l_1)$.

The factor $\delta^2\,\text{Re}(g)$ approximates the growth rates of the linear problem. Asymptotically it goes $\propto 1/\lambda^2$. The dashed line is the theoretical solution for the (effective) parameters from Table I. The growth rates are in qualitative agreement with simulations. However, quantitatively they are too small, as for a system somewhat closer to threshold. The solid curve represents the solution with 13% increased parameter β. This relatively small shift in one single parameter brings a good match with simulations. Important for the properties of the solution to Eqs. (17) is the ratio $R = \text{Re}(l_2)/\text{Re}(l_1)$. For $R > -1$ the cubic terms can saturate the growth of linearly unstable modes. For $-1 < R < 1$ standing waves and for $R > 1$ traveling waves are the stable saturated solutions. The right panel of Fig. 2 shows this ratio versus wavelength. Asymptotically both terms go $\propto 1/\lambda^4$ and R approaches a value of 2. Thus in the model cubic terms are able to stabilize the growth of all modes and standing waves should be unstable in this system as is observed in the simulations (Fig. 1, see also [21]).

In Fig. 3 we compare the evolution of the oscillation amplitudes from a simulation with $\tau = 1.4$ and radial box width 150 m (symbols) to theory (solid lines). The 75 m mode is stable; its growth is triggered solely by the 150 m mode through nonlinearity. The theoretical solution uses the (effective) parameters of Table I, again with the additional shift in β. A solution for the 75 m mode follows

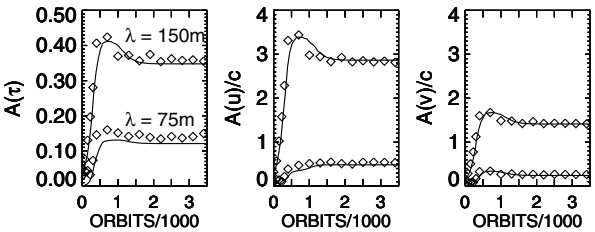

FIG. 3. Amplitudes of oscillations in the optical depth profile (left panel) and in the radial and tangential velocities (middle and right panels). The oscillation with $\lambda = 75$ m is excited as the harmonic of the 150 m mode. Symbols are values from simulations with $\tau = 1.4$; lines are results from the model using parameters from Table I with slightly enhanced β.

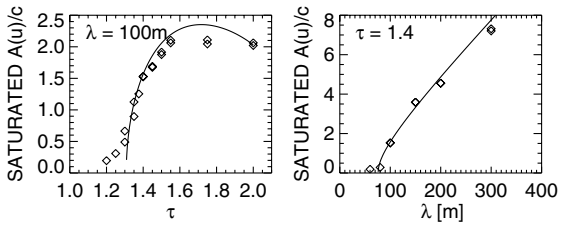

FIG. 4. Saturation amplitudes versus optical depth and wavelength. The solid line shows the results from the model; symbols are values determined from simulations.

from ψ_2. Saturation time scales and amplitudes are well reproduced by our model, for both primary and secondary modes. The hump around orbit 500 is connected to a transition from standing to traveling waves.

In Fig. 4 the saturation amplitudes are shown versus optical depth and wavelength. Again, if β is enhanced by 13% (solid line) theory and simulation are in good agreement. The decrease of the saturation amplitude for $\tau > 1.7$ is due to the fact that the critical wavelength increases in this regime with τ and comes close to 100 m. In general, however, for large wavelengths, the distance of the system to threshold increases with τ.

To conclude, we have presented particle simulations of a planetary ring that show the spontaneous creation and evolution of oscillatory modes. The growth of the modes saturates and eventually longer wavelengths grow at the cost of smaller ones. In all simulations shown in this Letter traveling waves are the stable saturated solutions [23]. Further we developed a weakly nonlinear model, based on a multiscale expansion of hydrodynamic equations. Considering the simplifications and approximations that were necessary to obtain an analytically treatable model, our theory gives a good description of the instability and saturation process seen in the simulations.

Clearly, simulational and theoretical approaches both give an idealized description of the particle flow of a planetary ring. But together they demonstrate the principles of an instability mechanism that has also been observed in more realistic configurations with particle size distribution and true particle-particle self-gravity (see [13]), and, most probably, is an ongoing dynamical process in planetary rings. The results of our study lend strong support to the idea that sub-km structure in the dense parts of Saturn's rings is caused by viscous overstability of the flow. It should be possible to identify the characteristic patterns and the time scales of overstable waves in the CASSINI imaging and occultation data. For an overstable system with $\tau \sim 2$ the group velocity is roughly $1/(20[\lambda/100\ \mathrm{m}]^2)$ wavelengths per orbit (about 10 h in the middle of Saturn's B ring). The study of further instabilities of the oscillatory state, with a possible radial variability of the oscillation amplitude, could eventually offer explanation for larger structures found in the Voyager data of the B ring.

We thank Larry Esposito, Arkady Pikovsky, and Frank Spahn for valuable comments. We acknowledge support by Deutsche Forschungsgesellschaft, the Ministerium für Forschung in Brandenburg, the Deutsche Akademische Austauschdienst, and the Academy of Finland.

[1] A. Lane, C. Hord, R. West, L. Esposito, D. Coffeen, M. Sato, K. Simmons, R. Pomphrey, and R. Morris, Science **215**, 537 (1982).
[2] J. N. Cuzzi, J. Lissauer, L. Esposito, J. Holberg, E. Marouf, G. Tyler, and A. Boischot, in *Planetary Rings*, edited by R. Greenberg and A. Brahic (The University of Arizona Press, Tucson, 1984), pp. 73–199.
[3] P. A. Rosen, G. L. Tyler, E. A. Marouf, and J. J. Lissauer, Icarus **93**, 25 (1991).
[4] C. K. Goertz and G. Morfill, Icarus **74**, 325 (1988).
[5] R. H. Durisen, N. L. Cramer, B.W. Murphy, J. N. Cuzzi, T. L. Mullikin, and S. E. Cederbloom, Icarus **80**, 136 (1989).
[6] S. Tremaine, astro-ph/0211149.
[7] J. Lukkari, Nature (London) **292**, 433 (1981).
[8] W. R. Ward, Geophys. Res. Lett. **8**, 641 (1981).
[9] S. Araki and S. Tremaine, Icarus **65**, 83 (1986).
[10] J. Wisdom and S. Tremaine, Astron. J. **95**, 925 (1988).
[11] U. Schmit and W. Tscharnuter, Icarus **115**, 304 (1995).
[12] U. Schmit and W. Tscharnuter, Icarus **138**, 173 (1999).
[13] H. Salo, J. Schmidt, and F. Spahn, Icarus **153**, 295 (2001).
[14] J. N. Cuzzi *et al.*, *Saturn's Rings: Pre-Cassini Status and Mission Goals*, http://ringmaster.arc.nasa.gov/ringpanel.
[15] M. K. Gordon *et al.*, in *The Future of Solar-System Exploration*, edited by M.V. Sykes (University of Arizona Press, Tucson, 2002), pp. 263–282.
[16] M. Cross and P. Hohenberg, Rev. Mod. Phys. **65**, 851 (1993).
[17] F. Bridges, A. Hatzes, and D. Lin, Nature (London) **309**, 333 (1984).
[18] H. Salo, Icarus **90**, 254 (1991).
[19] H. Salo, Nature (London) **359**, 619 (1992).
[20] P. Nicholson, R. French, E. Tollestrup, J. Cuzzi, J. Harrington, K. Matthews, O. Perkovic, and R. Stover, Icarus **145**, 474 (2000).
[21] J. Schmidt, H. Salo, F. Spahn, and O. Petzschmann, Icarus **153**, 316 (2001).
[22] A scalar product may be defined as $\langle\psi^{(1)}|\psi^{(2)}\rangle = \lim_{T\to\infty}\lim_{D\to\infty}\int_0^T dt\int_{-D}^{D} dx\psi^{(1)}\psi^{(2)}$.
[23] In systems with a stronger enhancement factor $\Omega_z/\Omega = 3.6$ we found a narrow belt of overstable wavelengths near the critical one, where standing waves were stable.